Inorganica Chimica Acta 362 (2009) 1455–1466

Contents lists available at ScienceDirect

Inorganica Chimica Acta

journal homepage: www.elsevier.com/locate/ica

Synthesis and NMR characterization of the novel mixed-ligand Pt(II) complexes *cis*- and *trans*-Pt(Ypy)(pyrimidine)Cl_2 and *trans*,*trans*-Cl_2(Ypy)Pt(μ-pyrimidine)Pt(Ypy)Cl_2 (Ypy = pyridine derivative)

Fernande D. Rochon *, Majd Fakhfakh

Chemistry Department, Université du Québec à Montréal, C. P. 8888, Succ. Centre-ville, Montréal, Canada H3C 3P8

ARTICLE INFO

Article history:
Received 31 May 2008
Accepted 4 July 2008
Available online 11 July 2008

Keywords:
Platinum complexes
Pyridine
Pyrimidine
X-ray crystal structure
NMR
IR

ABSTRACT

Mixed-ligand complexes of the type *cis*- and *trans*-Pt(Ypy)(pm)Cl_2 where Ypy = pyridine derivative and pm = pyrimidine were synthesized and characterized by IR spectroscopy and by multinuclear (^{195}Pt, ^{1}H and ^{13}C) magnetic resonance spectroscopy. The *cis* compounds were prepared from the reaction of K[Pt(Ypy)Cl_3] with pyrimidine (1:1 proportion) in water, while most of the *trans* isomers were synthesized from the isomerization of the *cis* compounds. The *cis* isomers could not be isolated with the Ypy ligands containing two –CH_3 groups in *ortho* positions. When the aqueous reaction of K[Pt(Ypy)Cl_3] with pyrimidine was performed in a Pt:pm ratio = 2:1, the pyrimidine-bridged dinuclear species were formed. Only the most stable *trans*–*trans* isomers could be isolated pure. In IR spectroscopy, the *cis* monomers showed two ν(Pt–Cl) bands, while the *trans* monomers and dimers showed only one ν(Pt–Cl) band. The ^{195}Pt NMR signals of the *cis* monomers were found at slightly higher fields than those of the corresponding *trans* isomers. The $\delta(^{195}Pt)$ of the dimers were found close to those of the *trans* monomers. The NMR results were interpreted in relation to the solvent effect, which seems important in these complexes. The coupling constants $J(^{195}Pt–^{1}H)$ and $J(^{195}Pt–^{13}C)$ are larger in the *cis* geometry. The crystal structures of the compounds *cis*-Pt(2,4-lut)(pm)Cl_2, *trans*-Pt(2,6-lut)(pm)Cl_2 and *trans*,*trans*-Cl_2(2,6-lut)Pt(μ-pm)Pt(Ypy)Cl_2 were studied by X-ray diffraction methods and the results have confirmed the configurations suggested by IR and NMR spectroscopies.

1. Introduction

The antitumor activity of cisplatin (*cis*-Pt$(NH_3)_2Cl_2$) has been known for decades and the compound is still one of the most commonly used drug for cancer treatment, even though its side effects are important. Its mechanism of action has been studied by several authors. It is extremely complex and there are still many uncertainties, although the antitumor properties are known to be related to a reaction with the bases (particularly guanine) of cellular DNA. A few good reviews have been published [1,2]. When the NH_3 ligands of cisplatin are replaced by pyridine (py), the compound *cis*-Pt$(py)_2Cl_2$ is not active, but the cytotoxicity of the *trans* isomer is comparable to the one of cisplatin in Leukemia L1210 cells [3]. The mixed-ligand compound *cis*-Pt(2-picoline)$(NH_3)Cl_2$ is quite active and it is in clinical trials [4,5]. The pyrazine-bridged dinuclear Pt(II) complex *cis*,*cis*-[Cl$(NH_3)_2$Pt(μ-pz)Pt$(NH_3)_2$Cl]Cl_2 was recently found to possess good anticancer properties and seems to overcome the cross-resistance of cisplatin [6]. The dinuclear compound has the appropriate Pt–Pt distance and the flexibility to react with a minimum of distorsion of the DNA molecule. A few other studies also indicate that dinuclear Pt(II) complexes might have a promising future in chemotherapy [7].

Pyrimidine (pm) is a diazine like pyrazine and can form bridges between two Pt atoms. A few pyrimidine-bridged-Pt(II) compounds were reported, like $K_2[Cl_3Pt(\mu\text{-pm})PtCl_3]$ and $Cl_2(R_2SO)Pt(\mu\text{-pm})Pt(R_2SO)Cl_2$ [8]. Pyrimidine and its derivatives are interesting molecules, since they play an important role in many biological processes. The molecule contains some empty π^* orbitals, which could accept electron density from a soft metal like Pt(II), but the nature of the Pt–pyrimidine bond has not yet been studied in the literature. However, only a few papers were published on platinum compounds with non-substituted pyrimidine. Fazakerley and Koch [9] synthesized and characterized *cis*-[Pt$(NH_3)_2(pm)_2$]$(ClO_4)_2$ by ^{13}C NMR spectroscopy while Rochon and coworkers [10] prepared *cis*- and *trans*-Pt$(pm)_2X_2$ (X = Cl and Br) and determined the crystal structures of the two *trans* isomers. Kaufmann et al. characterized *trans*-Pt$(PEt_3)(pm)Cl_2$ by ^{31}P and ^{1}H NMR, although they were not able to isolate the compound [11]. These authors also reported the pm-bridged compound *trans*,*trans*-Pt$(PBu_3)Cl_2$(μ-pm)Pt$(PBu_3)Cl_2$. More recently, we have published the synthesis of *cis*- and *trans*-Pt$(R_2SO)(pm)Cl_2$ [12], the dinuclear species $K_2[Cl_3Pt(\mu\text{-pm})PtCl_3]$ and $Cl_2(R_2SO)Pt(\mu\text{-pm})Pt(R_2SO)Cl_2$ (*cis*–*cis* and *trans*–*trans*) [8] and *trans*-Pt$(R_2SO)(pm)I_2$ [13,14].

---

* Corresponding author. Tel.: +1 514 987 3000/4896; fax: +1 514 987 4054.
E-mail address: rochon.fernande@uqam.ca (F.D. Rochon).

0020-1693/$ - see front matter © 2008 Elsevier B.V. All rights reserved.
doi:10.1016/j.ica.2008.07.003

We have now started a new study of mixed-ligand Pt(II) compounds containing a pyridine derivative (Ypy) and pyrimidine. Pyridine and its derivatives also contain empty π^* orbitals, which are able to accept electron density from the metal, but π-bonding does not seem to play an important role in the Pt–pyridine bond.

The Ypy ligands used in this work are unsubstituted pyridine, different picolines, (pic), lutidines (lut) and collidines (col). The influence of the methyl groups on Ypy was studied, especially when the methyl substituents are in *ortho* positions, where steric hindrance is quite important and is a major factor in the geometry of the mixed-ligand compounds. We have developed methods to synthesize *cis*- and *trans*-Pt(Ypy)(pm)Cl_2. The formation of pm-bridged dinuclear species was also studied. The new compounds were characterized by IR and multinuclear magnetic resonance spectroscopies. We have found that these techniques are usually good methods to determine the geometry of the different isomeric forms. A few compounds were also characterized by X-ray diffraction methods. The results of this study are reported below.

2. Experimental

$K_2[PtCl_4]$ was obtained from Johnson Matthey Inc. and was purified by recrystallization in water before use. Pyrimidine and the pyridine derivatives were obtained from Aldrich. $CDCl_3$ was purchased from CDN Isotopes, while CD_2Cl_2 was bought from Acros Organics.

The decomposition points were measured on a Fisher–Johns instrument and were not corrected. The IR spectra were recorded in the solid state (KBr pellets) on a FTIR Nicolet 4700 spectrometer between 4000 and about 280 cm^{-1}. All the NMR spectra were measured in $CDCl_3$ (except a few, which were measured in CD_2Cl_2) on a Varian Gemini 300BB spectrometer operating at 300.07, 75.460 and 64.267 MHz for ^1H, ^{13}C and ^{195}Pt, respectively. For ^{195}Pt, the external reference was $K_2[PtCl_4]$ in D_2O, adjusted at −1628 ppm from $K_2[PtCl_6]$ (δ(Pt) = 0 ppm).

2.1. Crystallographic studies

The crystals *cis*-Pt(2,4-lut)(pm)Cl_2 (**1**), *trans*-Pt(2,6-lut)(pm)Cl_2 (**2**) and *trans,trans*-Pt(2,6-lut)Cl_2(μ-pm)Pt(2,6-lut)Cl_2 (**3**) were mounted on a glass fiber using Paratone N hydrocarbon oil. Measurements were made at 200(2) K on a Bruker APEX II area detector diffractometer, equipped with graphite monochromated MoKα (λ = 0.71073 Å) radiation. Frames corresponding to an arbitrary hemisphere of data were collected using ω scans of 0.5° counted for a total of 30 s per frame. The program used for retrieving the cell parameters and data collection was APEX 2 [15]. The data were integrated using the program SAINT [16]. The data were corrected for Lorentz and polarization effects and a multiscan absorption correction was performed using the SADABS program [17]. The structures were solved and refined using SHELXS-97 and SHELXL-97 programs [18]. Crystal **2** was twinned with 20–80% proportions. All non-H atoms were refined anisotropically and the H positions were placed at idealized positions. Neutral atom scattering factors were taken from the International Tables for X-ray Crystallography [19]. All calculations and drawings were performed using the SHELXTL package [20]. The final model was checked for missing symmetry or voids in the crystal structure using the PLATON software [21]. The structures gave satisfactory checkcif reports. The crystal data and the most important experimental details are shown in Table 1.

2.2. Synthesis of the complexes

The K[Pt(Ypy)Cl_3] complexes were synthesized according to the methods described in the literature [22,23].

In the following data, the IR assignments are based on several papers in the literature [24], the vibration numbers are placed in parentheses and the frequencies are in cm^{-1}. The pyrimidine and ν(Pt–Cl) bands are shown in Tables 2 and 7. The chemical shifts in ^1H and ^{13}C NMR are listed in the Supplementary material.

Table 1
Crystal data and experimental details

	1	**2**	**3** · 2CHCl$_3$
Compound	*cis*-Pt(2,4-lut)(pm)Cl_2	*trans*-Pt(2,6-lut)(pm)Cl_2	{PtCl_2(2,6-lut)}$_2$(μ-pm)
Chemical formula	$C_{11}H_{13}Cl_2N_3Pt$	$C_{11}H_{13}Cl_2N_3Pt$	$C_{20}H_{24}Cl_{10}N_4Pt_2$
M_w	453.23	453.23	1065.11
Space group	$P2_1/n$	$P2_1/c$	$C2/c$
a (Å)	11.3334(7)	8.1614(9)	22.139(5)
b (Å)	9.9095(6)	7.8291(9)	7.6870(18)
c (Å)	11.9392(7)	21.1282(8)	21.372(5)
β (°)	91.646(1)	96.285(1)	120.405(2)
Volume (Å^3)	1340.33(14)	1341.9(2)	3136.9(13)
Z	4	4	4
$\rho_{calc.}$ (g cm^{-3})	2.246	2.243	2.255
μ (mm^{-1})	10.848	10.835	9.781
2θ Maximum (°)	52	52	54.00
Measured reflections	14082	3526	17621
Independent reflections (R_{int})	2621 (0.022)	2774	3405 (0.024)
Observer reflections	2397	2647	3178
R_1 ($I > 2\sigma(I)$)	0.0168	0.0414	0.0179
wR_2 (all data)	0.0416	0.1353	0.0444
S	1.081	1.121	1.021

2.2.1. *cis-Pt(Ypy)(pm)Cl_2 (Ypy = py, 2-pic, 3-pic, 2,3-lut, 2,4-lut, 2,5-lut, 3,4-lut, 3,5-lut and 2,3,5-col)*

K[Pt(Ypy)Cl_3] (0.1 mmol) is dissolved in 0.5 mL of a 0.1 M NaCl solution and added dropwise (while stirring) to pyrimidine (0.11 mmol) dissolved in 4 drops of water. The mixture is filtered after 2 h and the residue is washed with water, dried, washed with diethylether, dried in air and finally dried under vacuum in a dessiccator. The compounds are light yellow.

cis-Pt(py)(pm)Cl_2: Yield = 42%, dec. 259–275 °C. IR ν(C–H) aromatic 3104sh, 3093w, 3085w, 3070vw, 3041w, 3026w, 3002vw, py (8a) 1606m, (19a) 1481w (19b) 1449w, (9a) 1242w, 1208w, (15) 1147sh, (18a) 1073m, (12) 1057w, (1) 1019w, (10b) 776sh, 765 m, (4) 689sh, (16b) 462w, other bands 1220w, 982vw, 957vw.

cis-Pt(3-pic)(pm)Cl_2: Yield = 70%, m.p. 127–140 °C, dec. 255–280 °C. IR ν(C–H) aromatic 3109sh, 3095w, 3073m, 3061m, 3037sh, 3009vw, 3-pic $\nu_{as}(CH_3)$ 2959sh, 2948vw, $\nu_s(CH_3)$ 2927w, $\delta_{as}(CH_3)$ 1449sh, $\delta_s(CH_3)$ 1384m, $\rho(CH_3)$ 1043w, (8a) 1607w, (8b) 1582sh, (19a) 1481m, (13) 1247w, (9a) 1187w, (15) 378w, 370w, (18a) 1073w, (12) 1034w, (18b) 1114m, (14) 1342w, (1) 1046w, (17a) 996w, (5) 934w, (10b) 809m, 798m, (11) 501w, (6b) 670w, (6a) 538vw, (16a) 427w, other bands 955vw, 919vw.

cis-Pt(2,3-lut)(pm)Cl_2: Yield = 61% m.p. 146–152 °C, dec. 265–270 °C. IR ν(C–H) aromatic 3121tw, 3088w, 3069w, 3052w, 3030tw, 3006tw, 2,3-lut $\nu_{as}(CH_3)$ 2987tw, 2960w, $\nu_s(CH_3)$ 2915w, 2905sh, $\delta_{as}(CH_3)$ 1450s, $\delta_s(CH_3)$ 1387m, $\rho(CH_3)$ 979w, (8a) 1590vs, (8b) 1578sh, (19a) 1466vsF, (19b) 1437sh, (10b) 805vs, 796sh, (4) 718m, (11) 525w, 518sh, (10a) 447w, other bands 1366w, 1267sh, 1262w, 1245w, 1193vw, 1080m, 1069w, 1019sh, 988w, 935vw, 762vw, 614vw, 485vw, 371w.

cis-Pt(2,4-lut)(pm)Cl_2: Yield = 83%, m.p. 146–150 °C, dec. 258–260 °C. IR ν(C–H) aromatic 3118vw, 3096w, 3070w, 3057w, 3035w, 3007w, 2,4-lut $\nu_{as}(CH_3)$ 2984w, 2957w, $\nu_s(CH_3)$ 2919w, $\delta_{as}(CH_3)$ 1450m, $\delta_s(CH_3)$ 1376w, $\rho(CH_3)$ 1036m 995vw, (8a) 1625s, 1618sh, (8b) 1579sh, (19a) 1492w, 1485w, (10b) 812m, (4) 723w, (11) 545w, (10a) 459w, 449w, other bands 1359w, 1346sh, 1301w, 1272w, 1240vw, 1185vw, 1072w, 1036w, 974vw, 929w, 893w, 752vw, 572vw, 559vw, 374w, 314w.

cis-Pt(2,5-lut)(pm)Cl_2: Yield = 59%, m.p. 143 °C, dec. 238–258 °C. IR ν(C–H) aromatic 3122vw, 3097w, 3087vw, 3064w,

Table 2
Tentative assignment of the pyrimidine vibration modes in *cis*- and *trans*-Pt(Ypy)(pm)Cl_2

Mode	Free pm [24d]	py	3-pic	2,3-lut	2,4-lut	2,5-lut	3,4-lut	3,5-lut	2,3,5-col	2,6-lut	2,4,6-col	2,3,6-col
8b	1576	1589vs	1592vs	1590vs	1592vs	1590vs	1592sh	1593vs	1590vs	1593s	1592s	1593vs
8a	1566	1551m	1556m	1558m	1557s	1553m	1557s	1556m	1560s	1559m	1558m	1557m
19b	1476	1463w	1469m	1466vs	1467m	1461m	1469s	1469m	1468s			1477s
19a	1403	1407vs	1409vs	1408vs	1404vs	1404vs	1405vs	1408vs	1410vs	1408vs 1400m	1406vs	1407vs
3	1237	1227w	1225w	1228w	1223w	1220w	12vs	1226w	1231m	1223w	1226w	1221w
15	1161	1174w	1174w	1175w	1174w	1172w	1171m	1176w	1177w	1163m	1176w	1175w
9a	1143	1131w	1133w	1138m 1132sh	1126w	1128vw	1133vw 1128vw	1136vw	1137w	1134vw		1132vw
18b	1084	1090vw	1091vw	1091w	1089vw	1086vw	1089m	1092vw		1094w	1091vw	1094w
12	1064	1057m	1060w	1056m	1060m	1058w	1060m	1059w	1058m	1061w	1060w	1060w
1	991	1027w	1029w	1028m	1030m	1028m	1027m	1028w	1031m	1031m	1030w	1029w
10b	832	827w 820w	826sh	823m 815m	832s	819s	812s	819m 805w	827m	816m	815m	818m
4	721	706sh 697s	702vs	699vs	701vs	704vs	701vs	707s 699s	704vs	700vs	701s	702s
6a	676		685sh	685sh	685sh	684w	684w	684sh	685sh	682sh	684w	684w
6b	642	642w	643m	643m	644m	642m	643m	643m	646m	644m	644w	643w
ν(Pt–Cl)		345m 334m	337s 331s	342s 335s	340s 330s	339s	344vs 336vs	336m 329m	331s 327s	340s	354m	341m

3051w, 3038w, 3012vw, 3000vw, 2,5-lut $\nu_{as}(CH_3)$ 2985vw, 2979vw, 2960vw, $\nu_s(CH_3)$ 2925tw, 2912sh, $\delta_{as}(CH_3)$ 1449sh, $\delta_s(CH_3)$ 1384m, $\rho(CH_3)$ 1043w, 1012sh, 973w, (8a) 1616w, (8b) 1575w, (19a) 1499vs, (19b) 1429w, (10b) 832sh, (4) 720w, (11) 517sh, 510m, (10a) 458w, 446w, other bands 1366tw, 1357sh, 1349w, 1260vw, 1224sh, 1247w, 1142w, 1070w, 1034w, 983w, 916vw, 845w, 675vw, 372w.

cis-Pt(3,4-lut)(pm)Cl_2: Yield = 81%, m.p. 145–152 °C, dec. 262–270 °C. IR ν(C–H) aromatic 3115vw, 3088w, 3068w, 3050w, 3007vw, 3,4-lut $\nu_{as}(CH_3)$ 2978w, 2954w, 2946w, $\nu_s(CH_3)$ 2924w, 2905sh, $\delta_{as}(CH_3)$ 1453m, 1445m, $\delta_s(CH_3)$ 1384m, $\rho(CH_3)$ 1045vw, 1020w, 1001sh. (8a) 1616m, (19a) 1492s, (19b) 1425sh, (10b) 833s, (4) 714m, (11) 551w, (10a) 431w, other bands 1363w, 1351sh, 1304sh, 1251w, 1207w, 1175sh, 1074w, 995vw, 966vw, 890w, 755vw, 620w, 530vw, 378w, 319sh.

cis-Pt(3,5-lut)(pm)Cl_2: Yield = 67%, color change at 247 °C, dec. 270–295 °C. IR ν(C–H) aromatic 3116vw, 3095sh, 3080w, 3069w, 3046sh, 3036sh, 3010vw, 3,5-lut $\nu_{as}(CH_3)$ 2991vw, 2977vw, 2949vw, $\nu_s(CH_3)$ 2919w, $\delta_{as}(CH_3)$ 1445sh, $\delta_s(CH_3)$ 1385w, $\rho(CH_3)$ 1047w, (8b) 1579sh, (19b) 1435sh, (10b) 867m, (11) 509sh, 499w, (10a) 451vw, 431vw, other bands 1378sh, 13634vw, 1282vw, 1254w, 1156w, 1078vw, 985vw, 942vw, 380vw.

cis-Pt(2,3,5-col)(pm)Cl_2: Yield = 16%; color change 167 °C, dec. 265–275 °C. IR ν(C–H) aromatic 3097m, 3074m, 3035w, 3010w, 2,3-lut $\nu_{as}(CH_3)$ 2976vw, 2953w, $\nu_s(CH_3)$ 2922w, $\delta_{as}(CH_3)$ 1459w, $\delta_s(CH_3)$ 1388w, $\rho(CH_3)$ 1031m, 1006w, (8a) 1613w, (8b) 1576w, (19a) 1477w, (10b) 881m, 871sh, (4) 716m, (11) 534w, other bands 1545w, 1437w, 1356m, 1255w, 1215w, 1151w, 951vw, 790w, 745vw, 557vw, 507w, 344sh.

2.2.2. *trans*-Pt(Ypy)(pm)Cl_2 (Ypy = py, 2-pic, 3-pic, 2,3-lut, 2,4-lut, 2,5-lut, 3,4-lut, 3,5-lut and 2,3,5-col)

These complexes were prepared from the isomerization of the *cis* analogues in chloroform at 40 °C. The reaction takes a few weeks and the product always contains a small quantity of dimers *trans,trans*-Cl_2(Ypy)Pt(μ-pz)Pt(Ypy)Cl_2, Pt$(Ypy)_2Cl_2$ and Pt$(pm)_2Cl_2$. Therefore the IR spectra of the complexes were not recorded. The NMR signals of the impurities were removed from the data shown in the Supplementary material.

2.2.3. *trans*-Pt(Ypy)(pm)Cl_2 (Ypy = 2,6-lut, 2,3,6-col and 2,4,6-col)

The salt K[Pt(Ypy)Cl_3] (0.1 mmol) is dissolved in 0.5 mL of a NaCl (0.1 M) solution and added dropwise to pyrimidine (0.11 mmol) dissolved in 4 drops of the same solution. The mixture is stirred for 12 h and the mixture is then filtered. The yellow residue is washed with water, dried, washed with diethylether, dried in air and finally in a dessicator under vacuum.

trans-Pt(2,6-lut)(pm)Cl_2: Yield = 54%, color change at 247 °C, dec. 292–300 °C. IR ν(C–H) aromatic 3121vw, 3095w, 3082w, 3075w, 3061vw, 3050vw, 3037w, 3009vw, 2,6-lut $\nu_{as}(CH_3)$ 2987w, 2956w, $\nu_s(CH_3)$ 2923sh, 2914w, $\delta_{as}(CH_3)$ 1458sh, $\delta_s(CH_3)$ 1375m, 1370m, $\rho(CH_3)$ 1031m, (8a) 1611m, (8b) 1569w, (19a) 1473s, (19b) 1425m, (10b) 798s, 784sh, (4) 730sh, other bands 1499vw, 1432sh, 1360w, 1271vw, 1249vw, 1177w, 1119w, 1077vw, 1043vw, 1005w, 997w, 968vw, 946vw, 909vw, 539w, 375w.

trans-Pt(2,3,6-col)(pm)Cl_2: Yield = 34%, dec. 238–148 °C. IR ν(C–H) aromatic 3118vw, 3098w, 3083vw, 3076sh, 3072w, 3035w, 3009vw, 2,3,6-col $\nu_{as}(CH_3)$ 2977w, 2955w, 2949sh, $\nu_s(CH_3)$ 2920w, $\delta_{as}(CH_3)$ 1444w, $\delta_s(CH_3)$ 1388sh, 1377m, 1365w, $\rho(CH_3)$ 1029w, 994w, (8a) 1604m, (19a) 1472s, (19b) 1428w, (10b) 843w, 835w (4) 729vw, other bands 2860w, 1255vw, 1185sh, 1158w, 1152w, 1078vw, 1060w, 997vw, 994vw, 935vw, 787sh, 562w, 504w, 499w, 373vw, 319w.

trans-Pt(2,4,6-col)(pm)Cl_2: Yield = 10%, m.p. 103–135 °C, dec. 233–240 °C. IR ν(C–H) aromatic 3119tw, 3102w, 3095w, 3085w, 3070w, 3051w, 3036w, 3007tw, 2,4,6-col $\nu_{as}(CH_3)$ 2981w, 2959w, $\nu_s(CH_3)$ 2917w, $\delta_s(CH_3)$ 1375m, $\rho(CH_3)$ 1030w, (8a) 1627s, (19a) 1466s, (19b) 1428m, (10b) 855m, (4) 726w, other bands 2851w, 1246sh, 1152w, 1114vw, 895vw, 668vw, 548vw, 502vw, 376vw, 324w.

2.2.4. Cl_2(Ypy)Pt(μ-pm)Pt(Ypy)Cl_2 (Ypy = 2-pic, 3-pic, 2,3-lut, 2,4-lut, 2,5-lut, 3,4-lut, 2,3,5-col)

K[Pt(Ypy)Cl_3] (0.11 mmol) is dissolved in 1 mL of a NaCl solution (0.1 M), while pyrimidine (0.05 mmol) is dissolved in 3 drops in the same NaCl solution. The two solutions are stirred together for 2 days. The precipitate is filtered and washed with water. The product is then refluxed in dichloromethane for 25 to 35 days and filtered to remove the decomposed product. The filtrate was evaporated to dryness and the yellow residue washed with diethylether and dried under vacuum.

Cl_2(2-pic)Pt(μ-pm)Pt(2-pic)Cl_2: Yield 80%, color change at 140 °C, dec. 205–245 °C.

Cl_2(3-pic)Pt(μ-pm)Pt(3-pic)Cl_2: Yield 57%, color change at 130 °C, dec. 230–255 °C. IR ν(C–H) aromatic 3002sh, 3-pic $\nu_{as}(CH_3)$ 2962w, 2951sh, $\nu_s(CH_3)$ 2928sh, 2923vw, $\delta_{as}(CH_3)$ 1455w, $\delta_s(CH_3)$ 1376w, (8a) 1606w, (8b) 1580w, (19a) 1480w, (10b) 796s, 760sh, other bands 1538w, 1505w, 1260m, 1092m, 1016m, 668w, 660w, 503w, 492w, 412sh, 398vs, 385sh, 376sh, 357w, 337w, 326w.

Cl_2(2,3-lut)Pt(μ-pm)Pt(2,3-lut)Cl_2: Yield = 80%, color change at 102–118 °C, dec. 196–215 °C. IR ν(C–H) aromatic 3118w, 3108vw, 3090w, 3081sh, 3075sh, 3072sh, 3037vw, 2,3-lut $\nu_{as}(CH_3)$ 2963w, $\nu_s(CH_3)$ 2917vw, $\delta_{as}(CH_3)$ 1454s, $\delta_s(CH_3)$ 1374m, (8a) 1603s, (10b) 794s, (4) 717s, other bands 1366w, 1267sh, 1262w, 1245w, 1193w, 1080w, 1069w, 1028m, 1019sh, 988w, 935w, 762vw, 614w, 485w, 371w.

Cl_2(2,4-lut)Pt(μ-pm)Pt(2,4-lut)Cl_2: Yield 62%, dec. 150–165 °C. IR 2,4-lut $\nu_{as}(CH_3)$ 2993 sh 2979sh, 2963w, $\nu_s(CH_3)$ 2928w, 2915w, $\delta_{as}(CH_3)$ 1456w, $\delta_s(CH_3)$ 1377w, (8a) 1623w, (10b) 790s, other bands 2905w, 2877w, 2869w, 2840w, 1717vw, 1653vw, 1540vw, 1508vw, 1358sh, 1260w, 1095m, 1018m, 862w, 751sh, 667vw, 658vw, 562w, 546w, 507w, 451w, 394vs.

Cl_2(2,5-lut)Pt(μ-pm)Pt(2,5-lut)Cl_2: Yield = 76%, dec. 245–255 °C. IR 2,5-lut ν(C–H) aromatic 3127sh, 3124sh, 3119w, 3112sh, 3092w, 3081sh, 3077sh, 3073sh, 3048w, 3044w, 3039w, 2,5-lut $\nu_{as}(CH_3)$ 2975vw, 2972w, 2963vw, $\nu_s(CH_3)$ 2921w, $\delta_{as}(CH_3)$ 1457w, (8a) 1617w, (8b) 1575vw, (19a) 1500m, (19b) 1464w, (10b) 832s, other bands 2869w, 2861w, 1538vw, 1533sh, 1344w, 1266vw, 1246vw, 1226vw, 1217sh, 1186vw, 1112vw, 1030vw, 733w, 642vw, 514w, 452w.

Cl_2(3,4-lut)Pt(μ-pm)Pt(3,4-lut)Cl_2: Yield = 59%, color change at 122–130 °C, dec. 198–212 °C. IR ν(C–H) aromatic 3123vw, 3096vw, 3085vw, 3076vw, 3041vw, 3025vw, 3,4-lut $\nu_{as}(CH_3)$ 2991sh, 2962w, $\nu_s(CH_3)$ 2923w, $\delta_{as}(CH_3)$ 1450m, $\delta_s(CH_3)$ 1388w, (8a) 1604w, (19a) 1495m, (10b) 834m, 817sh, other bands 2870w, 2851w, 1377w, 1304vw, 1201w, 1168w, 1137w, 1123sh, 1089vs, 1045sh, 1022vs, 909w, 864w, 749m, 664w, 400w, 387w, 314w.

Cl_2(3,5-lut)Pt(μ-pm)Pt(3,5-lut)Cl_2: Yield = 25%, dec. 210–230 °C. IR ν(C–H) aromatic 3094vw, 3,5-lut $\nu_{as}(CH_3)$ 2963m, $\nu_s(CH_3)$ 2924w, $\delta_{as}(CH_3)$ 1456w, $\delta_s(CH_3)$ 1384w, (8a) 1604w, (8b) 1575w, (19a) 1464w, (10b) 863m, other bands 2907w, 1569w, 1521vw, 1506vw, 1261s, 1156sh, 1093s, 1019s, 693m, 668m, 660m, 504vw, 394s, 349s. Cl_2(2,3,5-col)Pt(μ-pm)Pt(2,3,5-col)Cl_2: Yield = 11%, dec. 150–165 °C.

Cl_2(2,3,5-col)Pt(μ-pm)Pt(2,3,5-col)Cl_2: Yield = 15%, dec. 150–165 °C.

2.2.5. *Cl_2(Ypy)Pt(μ-pm)Pt(Ypy)Cl_2 (Ypy = 2,6-lut and 2,4,6-col)*

Pyrimidine (0.05 mmol) dissolved in 3 drops of an NaCl 0.1 M solution was added to K[Pt(Ypy)Cl_3] (0.11 mmol) dissolved in 1 mL of the same solution. The mixture was stirred for five days. The pale precipitate was then filtered, washed with water, dried, washed with diethylether, dried in air and finally in a dessicator under vacuum.

Cl_2(2,6-lut)Pt(μ-pm)Pt(2,6-lut)Cl_2: Yield = 70%, color change at 120 °C, dec. 220–250 °C. IR ν(C–H) aromatic 3113w, 3095w, 3081w, 3052vw, 3030vw, 2,6-lut $\nu_{as}(CH_3)$ 2980w, 2954w, $\nu_s(CH_3)$, 2916w, (8a) 1610s, (8b) 1581w, (19a) 1474vs, (19b) 1427m, (10b) 782vs, other bands 2852w, 1567w, 1542vw, 1500vw, 1350w, 1253vw, 1186sh, 1137w, 1118vw, 1096w, 999w, 934w, 893vw, 738vw, 730w, 707vw, 501vw, 406w, 354m, 313w.

Cl_2(2,4,6-col)Pt(μ-pm)Pt(2,4,6-col)Cl_2: Yield = 33%, dec. 193–213 °C. IR ν(C–H) aromatic 3114vw, 3091w, 3045vw, 3025vw, 3003w, 2,4,6-col $\nu_{as}(CH_3)$ 2983w, 2955w, $\nu_s(CH_3)$ 2918w, $\delta_s(CH_3)$ 1375m, $\rho(CH_3)$ 1031w, (8a) 1627s, (8b) 1583sh, (19a) 1464s, (19b) 1428m, (10b) 852m, other bands 2850vw, 1507vw, 1226w, 1183w, 1173w, 1137w, 1085w, 1014w, 937vw, 897vw, 830w, 750m, 662w, 546w, 327m.

2.2.6. *Cl_2(2,3,6-col)Pt(μ-pm)Pt(2,3,6-col)Cl_2*

Pirimidine (0.05 mmol) dissolved in 3 drops of an NaCl 0.1 M solution is added very slowly to K[Pt(2,3,6-col)Cl_3] (0.11 mmol) dissolved in 1 mL of the same solution. The mixture is stirred during 5 days. The precipitate is filtered out, washed with water, dried, washed with diethylether and dried in air. The product is then dissolved in dichloromethane and filtered. The filtrate is evaporated to dryness and the yellow residue is washed with diethylether and dried under vacuum. Yield = 24%, color change at 190 °C, dec. 230–255 °C. IR ν(C–H) aromatic 3119w, 3087w, 3068sh, 3035vw, 2,3,6-col $\nu_{as}(CH_3)$ 2986w, 2955w, $\nu_s(CH_3)$ 2920w, $\delta_{as}(CH_3)$ 1444w, $\delta_s(CH_3)$ 1387m, 1377m, 1366sh, $\rho(CH_3)$ 1027w, (8a) 1604vs, (8b) 1583sh, (19a) 1475vs, (19b) 1428m, (10b) 822m, other bands 2868w, 2851w, 1348w, 1323sh, 1226w, 1152w, 1138w, 1090w, 970w, 935w, 897vw, 704vw, 665w, 645vw, 563w, 493vw, 423w, 402w, 317w.

3. Results and discussion

3.1. *Complexes Pt(Ypy)(pm)Cl_2*

3.1.1. *Synthesis*

The complexes *cis*-Pt(Ypy)(pm)Cl_2 (Ypy = py, 2-pic, 3-pic, 2,3-lut, 2,4-lut, 2,5-lut, 3,4-lut, 3,5-lut and 2,3,5-col) were synthesized from the aqueous reaction of K[Pt(Ypy)Cl_3] with pyrimidine (proportion 1:1) in the presence of NaCl. The Pt(II) salt is added slowly to the pyrimidine solution in order to always have an excess of pyrimidine to prevent the formation of pyrimidine-bridged species. The reaction is stopped after 2 h. In these conditions, only the *cis* isomer is produced, since the *trans* effect of the chloro ligand is larger than the one of the pyridine ligand.

$$K[Pt(Ypy)Cl_3] + pm \xrightarrow[H_2O]{NaCl} cis\text{-}Pt(Ypy)(pm)Cl_2 \downarrow + KCl$$

K[Pt(Ypy)Cl_3] is not very stable in water without the presence of NaCl. If the time of reaction is longer, *trans* isomers will be formed. The yields vary between 42 and 83%, except for the 2,3,5-col compound, which was isolated in lower yields. The subsequent characterization of the products has shown pure compounds except *cis*-Pt(2-pic)(pm)Cl_2, which contained a small quantity of the *trans* isomer. Attempts to isolate the 2-pic product at lower temperature in order to reduce the isomerization have slowed down the reaction, but mixtures of isomers were also obtained. The *cis* → *trans* isomerization is faster with 2-pic, because of the presence of a substituent in *ortho* position. If the time of reaction is increased, the thermodynamically more stable *trans* compound is formed in larger quantities.

The complexes *trans*-Pt(Ypy)(pz)Cl_2 (Ypy = py, 2-pic, 3-pic, 2,3-lut, 2,4-lut, 2,5-lut, 3,4-lut, 3,5-lut and 2,3,5-col) were prepared from the isomerization of the corresponding *cis* compound in chloroform at 40 °C. The reaction is very slow (few weeks) and the products are always contaminated by the complexes *trans*-Pt(Ypy)$_2Cl_2$ [25], a small quantity of *trans*-Pt(pm)$_2Cl_2$ [10] and the dinuclear compound Cl_2(Ypy)Pt(μ-pm)Pt(Ypy)Cl_2 (to be discussed later in the text). All these neutral compounds have similar solubilities and could not be separated.

The complexes *trans*-Pt(Ypy)(pm)Cl_2 (Ypy = 2,6-lut, 2,3,6-col et 2,4,6-col) were prepared pure by the reaction described above to synthesize the *cis* isomers, but the time of reaction was longer (~12 h). The *cis* isomer is first formed since the *trans* effect of the chloro ligand is larger than the one of the pyridine derivative, but it rapidly isomerizes to the *trans* isomer because of steric hindrance caused by the presence of two –CH_3 groups in *ortho* positions.

$$K[Pt(Ypy)Cl_3] + pm \xrightarrow[-KCl]{H_2O} cis\text{-}Pt(Ypy)(pm)Cl_2(\text{cannot be isolated})$$
$$\rightarrow trans\text{-}Pt(Ypy)(pm)Cl_2$$

If the time of reaction is longer than 12 h, dinuclear species will be formed. The yields are lower (ave. 33%) than those of the *cis* isomers.

3.1.2. IR spectroscopy

The IR spectrum of free pyrimidine (C_{2v}) was published [24a,24b,24c,24d]. There are 22 vibration modes (A_1, B_1 and B_2) which are active in IR spectroscopy, while the two other modes (A_2) are active in Raman only. Coordination of pyrimidine to a metal reduces its symmetry to C_s and all the vibration modes are now active in IR [26]. Four of these vibrations are mainly stretching ν(C–H) vibrations. There is no IR study in the literature on Pt–pyrimidine complexes.

The IR spectra of only the pure compounds were recorded. A tentative assignment of bonded pyrimidine is shown in Table 2. In the 1630–1400 cm^{-1} region, the stretching ν(C–C) and ν(C–N) modes (8a, 8b, 19a, 19b) coupled to deformation δ(C–H) modes are strong bands. There are several weak bands between 1250 and 1200 cm^{-1}, one was assigned to the 3 mode. The region 1200–900 cm^{-1} contains the deformation modes in the heterocyclic plane, where the modes 9a, 15, 12, 18a and 1 were assigned. Mode 1 is the vibration of the complete aromatic ring, while 10b is the umbrella mode (1 or 2 bands) and 4 is the intense out of plane vibration mode. The 6a and 6b modes are out of plane deformations.

The Ypy bands are shown in the experimental section and the assignments are based on several literature reports [24]. The deformation modes $\delta_{as}(CH_3)$ were found around 1450 cm^{-1}, while the $\delta_s(CH_3)$ were observed at lower energies (1387–1365 cm^{-1}).

IR spectroscopy seems a good method to determine the geometry of these compounds. Two stretching ν(Pt–Cl) bands (A_1 and B_1, C_{2v} skeleton symmetry) are observed for the *cis* compounds between 327 and 345 cm^{-1}, while only one band (B_{3u}, D_{2h} skeleton symmetry) was detected between 339 and 354 cm^{-1} for the *trans* isomers.

3.1.3. Multinuclear magnetic resonance spectroscopy

The ^{195}Pt NMR spectra of all the compounds were measured in $CDCl_3$. There are only three ^{195}Pt NMR papers in the literature on Pt-pm compounds. These are on the complexes *cis* and *trans*-$Pt(R_2SO)(pm)Cl_2$ [12], *trans*-$Pt(R_2SO)(pm)I_2$ [13], $K_2[Cl_3Pt(\mu\text{-pm})PtCl_3]$ and $Cl_2(R_2SO)Pt(\mu\text{-pm})Pt(R_2SO)Cl_2I_2$ [8]. The chemical shifts ($\delta(^{195}Pt)$) of the compounds $Pt(Ypy)(pm)Cl_2$ are shown in Table 3. The *cis* compounds are pure (also confirmed by ^{1}H and ^{13}C NMR), except *cis*-$Pt(2\text{-pic})(pm)Cl_2$. The *trans* compounds containing Ypy = 2, 6-lut, 2,3,6-col et 2,4,6-col are also pure, but those prepared from the isomerization of the *cis* compounds contain other impurities as discussed above. The assignments for the latter *trans* compounds were made at the beginning of the isomerization process, when there were only *cis*- and *trans*-$Pt(Ypy)(pm)Cl_2$.

The $\delta(^{195}Pt)$ vary between −2026 and −2054 for the *cis* isomers and between −1966 and −2014 ppm for the *trans* analogues. The signal of the *cis* compounds was found at higher field than the one of the corresponding *trans* analogue. The average difference between the two isomers ($\Delta\delta_{trans-cis}$) is 38 ppm. The complexes listed in Table 3 were separated into 3 different groups depending on the Ypy ligands. The complexes of group 1 contain pyridine derivatives which do not have any substituent in *ortho* positions, while those of group 3 contain Ypy with two $-CH_3$ substituents in *ortho* positions. In the group 2 compounds, the Ypy ligand has only one $-CH_3$ substituent in *ortho* position. The difference ($\Delta\delta_{trans-cis}$) seems slightly larger for group 2 compounds (41 ppm) than for group 1 (35 ppm). For the complexes $Pt(Ypy)_2Cl_2$, the $\Delta\delta$ value is about 52 ppm [25]. A smaller difference for the mixed-ligand complexes $Pt(Ypy)(pm)Cl_2$ might indicate the presence of a slightly stronger π-bond between pyrimidine and Pt(II) than between pyridine and Pt(II).

Table 3
$\delta(^{195}Pt)$ and $\Delta\delta_{trans-cis}$ (ppm) of $Pt(Ypy)(pm)Cl_2$ and the pK_a of protonated Ypy

Ypy	pK_a [27]	*cis*	*trans*	$\Delta\delta_{trans-cis}$
py	5.22	−2041	−2008	33
3-pic	5.63	−2040	−2005	35
3,4-lut	6.46	−2042	−2005	37
3,5-lut	6.15	−2041	−2007	34
Ave. gr. 1		*−2041*	*−2006*	*35*
2-pic	5.96	−2052	−2012	40
2,3-lut	6.57	−2029	−1983	46
2,4-lut	6.63	−2047	−2006	41
2,5-lut	6.40	−2054	−2014	40
2,3,5-col		−2026	−1987	39
Ave. gr. 2		*−2042*	*−2000*	*41*
2,6-lut	6.72		−1992	
2,4,6-col	7.48		−1987	
2,3,6-col	7.40		−1966	
Ave. gr. 3			*−1982*	

There is no relation between the $\delta(^{195}Pt)$ and the pK_a values [27] of the protonated pyridine derivative. The most basic ligands are the collidines, which should form stronger σ (ligand → Pt) bonds and the complexes should be observed at higher fields than the other compounds. In fact, the compounds of group 3 are observed at lower fields than the others. Therefore the electron density on the Pt atom is lower in group 3 compounds than in the others. Unfortunately, we cannot prepare *cis* complexes with pyridine derivatives containing two $-CH_3$ substituents in *ortho* position because of steric hindrance, but we can compare the results obtained in the *trans* series. We explain these results by the solvent effect, as suggested in the compounds $K[Pt(Ypy)Cl_3]$, which were studied in D_2O [23]. Chloroform is not as good as water as a coordinating solvent, but its influence should not be neglected. The molecules of solvent normally approach the Pt(II) atom on both sides of the square plane, which increases the electron density in the close environment of the metal atom, resulting in a ^{195}Pt chemical shift towards higher fields. When one of the ligand is a pyridine derivative containing two $-CH_3$ substituents in *ortho* position, the planar ligand will be perpendicular to the Pt(II) plane, in order to reduce steric hindrance with the *cis* neighbours. In this conformation, the two $-CH_3$ substituents will be above and below the coordination plane, directly above and below the Pt atom, which will reduce the approach of the molecules of solvent. The electron density on the metal atom will thus be reduced, which will cause the ^{195}Pt signal to shift towards lower field, as observed in our group 3 complexes.

It is interesting to note that the complexes containing Ypy with $-CH_3$ substituents in both positions 2 and 3 (2,3-lut, 2,3,5-col and 2,3,6-col) are observed at slightly lower field than the other complexes of their respective group.

The symmetry of free pyrimidine is C_{2v}. Its proton chemicals shifts are: H2 9.226, H4 and H6 8.737 and H5 7.328 ppm in $CDCl_3$. This order can be explained by the different ionic resonance structures and by the inductive effect of the N atoms. H5 is a doublet of triplet with ^3J(Pt–H4,6) = 4.9 Hz and ^5J(Pt–H2) = 1.59 Hz, H4,6 is a doublet and H2 is a singlet. The presence of the two neighboring N atoms with strong quadrupolar magnetic moments is probably responsible for the absence of couplings on H2.

The binding of pyrimidine to Pt(II) in a monodentate fashion reduces its symmetry to C_s and all the H atoms are different as shown in Scheme 1. Therefore 4 different signals are observed in ^{1}H NMR.

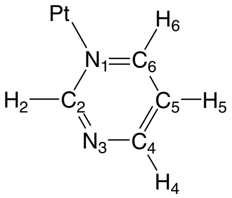

Scheme 1.

In the complexes Pt(Ypy)(pm)Cl_2, the signal of H2 is a doublet of doublets with $^5J(^1H2–^1H5)$ and $^4J(^1H2–^1H6)$ are ~1.2 Hz. It is not always seen because of the presence of the two neighbouring N atoms. It does not couple with H4, probably because of the presence of the non-coordinated N3 atom between the two atoms. The signal of H4 is a doublet of doublets with $^3J(^1H4–^1H5)$ ~4.8 Hz and $^4J(^1H4–^1H6)$ ~2.1 Hz. H5 is also a doublet of doublets with $^3J(^1H5–^1H6)$ ~6.0 Hz. Finally, the signal of H6 is a doublet of doublets of doublets, since it couples with H2, H4 and H5. This coupling pattern has also been observed in the complexes *cis*- and *trans*-Pt(R_2SO)(pm)Cl_2 [12].

The signals of pyrimidine have shown a downfield shift upon coordination, since the formation of the σ bond reduces the electron density on the ligand, while it is increased on the Pt atom. The chemical shifts differences $\Delta\delta(\delta_{\text{ligand}} - \delta_{\text{free pm}})$ (where the spectrum of free pm was measured in the same solvent) are shown in Table 4. The values of H2 for the *cis* isomers do not follow the expected pattern. The H–H coupling patterns of these atoms are different, therefore the assignments seem correct. A large downfield shift is observed for H6 (ave. $\Delta\delta$ = 0.753 ppm), while the position of H2 is almost not affected by coordination in the *cis* isomers. For the *trans* complexes, the expected values are observed. The signals of H2 and H6 are deshielded by ~0.42 ppm, while those of H4 and H5 are not very affected. The assignments in the *cis* and *trans* isomers were confirmed by 2D ^1H NMR studies.

In the *trans* isomers, the deshielding order is H2 > H6 > H4 > H5, while in the *cis* isomers, it is H6 > H2 > H4 > H5. In the complexes *cis*-et *trans*-Pt(R_2SO)(pm)Cl_2 (measured in CD_2Cl_2) [12], the order was the same for the two isomers (H2 > H6 > H4 > H5). In the latter complexes, the ave. $\Delta\delta$ are H2 = 0.217, H6 = 0.255 ppm (*cis*), and H2 = 0.304, H6 = 0.313 ppm (*trans*), except for *cis*-Pt(dibenzylsulfoxide)(pm)Cl_2, where all the signals were observed at higher fields than in free pyrimidine. In the ionic compound *cis*-[Pt$(NH_3)_2(pm)_2$]$(ClO_4)_2$, the $\Delta\delta$ values are: H2 = 0.45 ppm and H6 = 0.36 ppm in D_2O [9]. It seems therefore that our results on the *cis* compounds are the first example where the order of the chemical shifts of H2 and H6 is reversed upon coordination.

Table 4
$\Delta\delta$ (ppm) and ^3J(Pt–H) (Hz) of pm in Pt(Ypy)(pm)Cl_2

Ypy		H2	H4	H5	H6	ave.	^3J(Pt–H2)	^3J(Pt–H6)
Free pm		9.226	8.737	7.328	8.737			
py	*cis*	–0.055	0.048	0.127	0.644	0.191	22	40
	trans	0.407	0.039	[a]	0.403		19	33
3-pic	*cis*	–0.032	0.034	0.162	0.824	0.252	23	42
	trans	0.403	0.045	0.043	0.399	0.223		
3,4-lut	*cis*	–0.024	0.005	0.167	0.941	0.272		42
	trans	0.402	0.035	0.032	0.401	0.218	18	29
3,5-lut	*cis*	–0.047	0.025	0.161	0.855	0.249	24	42
	trans	0.403	0.044	[b]	0.397		19	
Ave. gr. 1	*cis*	*–0.040*	*0.028*	*0.154*	*0.816*	*0.240*	*23*	*42*
	trans	*0.404*	*0.041*	*0.038*	*0.400*	*0.221*	*19*	*31*
2-pic	*cis*	–0.077	0.027	0.130	0.642	0.181	22	42
	trans	0.441	0.046	0.039	0.440	0.242	19	
2,3-lut	*cis*	–0.078	0.009	0.159	0.738	0.207	23	38
	trans	0.448	0.048	0.039	0.444	0.245	18	32
2,4-lut	*cis*	–0.075	0.013	0.133	0.688	0.190	23	39
	trans	0.433	0.073	0.029	0.434	0.242	19	32
2,5-lut	*cis*	–0.093	0.034	0.140	0.657	0.185	25	43
	trans	0.439	0.048	0.039	0.436	0.241	22	33
2,3,5-col	*cis*	–0.095	0.010	0.201	0.790	0.227	24	39
	trans	0.442	0.040	0.031	0.442	0.239	17	32
Ave. gr. 2	*cis*	*–0.084*	*0.019*	*0.153*	*0.703*	*0.197*	*23*	*40*
	trans	*0.441*	*0.051*	*0.035*	*0.439*	*0.242*	*19*	*32*
2,6-lut	*trans*	0.460	0.048	0.037	0.465	0.253	19	33
2,4,6-col	*trans*	0.455	0.042	0.027	0.460	0.246	18	33
2,3,6-col	*trans*	0.467	0.049	[b]	0.472		19	30
Ave. gr. 3	*trans*	*0.461*	*0.046*	*0.032*	*0.466*	*0.251*	*19*	*32*

[a] Hidden by impurities.
[b] Hidden by H4 of Ypy.

Table 4 shows also the ave. $\Delta\delta$ values for each group of compounds. The values seem to slightly increase from group 1 to group 3 in the *trans* isomers. The influence of the $-CH_3$ substituents in *ortho* positions on the pyridine ligand located in *trans* position seems to affect the electron density on the protons of the pyrimidine ligand. In the *cis* compounds, the steric hindrance is the most important factor.

The proton coupling constants with ^{195}Pt could be measured for most of the compounds and they depend on the geometry (Table 4). The $^3J(^{195}Pt–^1H6)$ values are much larger in the *cis* compounds (41 Hz) than in the *trans* isomers (32 Hz). The $^3J(^{195}Pt–^1H2)$ values are also larger in the *cis* geometry (23 Hz vs. 19 Hz), although the difference is much smaller. Similar values were observed for *cis*- and *trans*-Pt(R_2SO)(pm)Cl_2 [12], and *trans*-Pt(R_2SO)(pm)I_2 [13].

The proton chemical shifts of the pyridine ligands are shown in the Supplementary material and the $\Delta\delta$ values are listed in Table 5. The average $\Delta\delta$ values for the three groups of complexes are also shown in the table. All the signals are shifted towards lower field upon coordination. It is difficult to compare the signals of the different Ypy ligands because of the local effects caused by the presence of methyl groups in different positions. The most deshielded atoms are the $-CH_3$ protons located in *ortho* positions, followed by H6.

For the *trans* complexes, the values seem to increase from group 1 to group 3. The latter group contains the most basic ligands. These results are therefore in agreement with the pK_a values of the protonated ligands. The strength of the σ bond should be larger in the group 3 complexes, thus the electron density on the Ypy ligand should be smaller for this group. For the *cis* compounds, the trend seems similar, although steric hindrance should play a more important role.

Several $^3J(^{195}Pt–^1H)$ couplings were observed. They vary from 36 to 42 Hz (ave. 38 Hz) for the *cis* isomers and between 27 and 33 Hz (ave. 30 Hz) for the *trans* analogues. It seems therefore that this value is a good criterion to determine the geometry of these complexes. A few couplings $^4J(^{195}Pt–^1H)$ could also be measured and they vary between 10 and 12 Hz. Similar values were observed for the compounds Pt$(Ypy)_2Cl_2$ [25].

As in ^1H NMR, four signals will be observed in ^{13}C NMR for Pt-bonded pyrimidine. The $\Delta\delta$ values ($\delta_{\text{pm}} - \delta_{\text{free pm}}$ in $CDCl_3$) are shown in Table 6. The *trans* compounds obtained from the isomerization of the *cis* isomers showed the presence of other Pt complexes, which could be substracted from the spectra only for a few ligands. The compound *trans*-Pt(2,3-lut)(pm)Cl_2 was accidentally obtained pure when the reaction of K[Pt(2,3-lut)Cl_3] and pyrimidine was performed in a very large excess of NaCl. This result could not be reproduced with the other ligands.

All the pm signals were observed at lower field than those of free pyrimidine. The $\Delta\delta$ values are larger for C6. The main differences between the *cis* and *trans* isomers are in the position of C2 and C5. The signal of C2 is more shielded in the *cis* compounds (ave. $\Delta\delta$ values = 1.16 vs. 2.53 ppm), while the one of C5 is more shielded in the *trans* isomers (ave. $\Delta\delta$ values = 0.12 vs. 1.66 ppm). The total average values of the four C atoms are very similar in the two geometries. Therefore the total electron density on the four C atoms of the pm ligand seems identical in the two isomers. In the series Pt(R_2SO)(pm)Cl_2 [12], all the C atoms are more deshielded in the *cis* geometry, probably because π-bonding is more important in the R_2SO-pm complexes and it is more effective in the *cis* geometry.

The average $\Delta\delta$ values were calculated for the three different groups of Ypy ligands and the results are shown in Table 6. These values were compared with the $\delta(^{195}Pt)$ and there is an agreement, although there are few results on some groups of complexes. In the

Table 5
$\Delta\delta$ (ppm) and $J(^{195}Pt–^{1}H)$ (Hz) for Ypy in $Pt(Ypy)(pm)Cl_2$

Ypy		H2	2Me	H3	3Me	H4	4Me	H5	5Me	H6	6Me	^3J(Pt–H2/6)		^4J(Pt–H2,6–Me)
												H2	H6	
Pyridine	*cis*	0.262		0.137		0.208		0.137		0.262		36	36	
	trans	0.310		0.108		0.186		0.108		0.310		30	30	
3-pic	*cis*	0.277			−0.028	0.112		0.024		0.239			42	
	trans				0.032	0.101								
3,4-lut	*cis*	0.314			−0.004		0.049	0.073		0.303				
	trans	0.258			0.060		0.102	0.076		0.240		27		
3,5-lut	*cis*	0.239			−0.038	0.079			0.038	0.239		36	36	
	trans	0.194			0.027				0.027	0.194		31	31	
Ave. gr. 1	*cis*	*0.273*		*0.137*	*0.023*	*0.160*	*0.049*	*0.105*	*0.038*	*0.268*				
	trans	*0.226*		*0.108*	*0.040*	*0.144*	*0.102*	*0.092*	*0.027*	*0.248*				
2-pic	*cis*		0.603			0.149								
	trans		0.713	0.165		0.089		0.101		0.371				
2,3-lut	*cis*		0.799		0.088	0.165		0.169		0.842			40	
	trans		0.849		0.111	0.127		0.084		0.450			33	11
2,4-lut	*cis*		0.566	0.150			0.057	0.169		0.705			40	11
	trans		0.680	0.133			0.080	0.072		0.320			33	
2,5-lut	*cis*		0.631	0.225		0.168			0.086	0.687			36	12
	trans		0.750	0.190		0.115			0.092	0.425			27	
2,3,5-col	*cis*		0.780		0.049	0.161			0.060	0.731			36	
	trans		0.894		0.075	0.128			0.087	0.474			29	
Ave. gr. 2	*cis*		*0.676*	*0.188*	*0.069*	*0.161*	*0.057*	*0.169*	*0.073*	*0.741*				
	trans		*0.777*	*0.162*	*0.093*	*0.115*	*0.080*	*0.076*	*0.090*	*0.408*				
2,6-lut	*trans*		0.906	0.198		0.081		0.198			0.906			11
2,4,6-col	*trans*		0.907	0.209			0.127	0.209			0.907			10
2,3,6-col	*trans*		0.977		0.112	0.130		0.181			1.045			
Ave. gr. 3	*trans*		*0.930*	*0.204*	*0.112*	*0.106*	*0.127*	*0.196*			*0.953*			

Table 6
$\Delta\delta(^{13}C)$ (ppm) of pm in *cis*- and *trans*-$Pt(Ypy)(pm)Cl_2$

Ypy	Geometry	C2	C4	C5	C6	Ave.
Free pm		159.06	156.78	121.42	156.78	
py	*cis*	1.18	1.45	1.56	3.38	1.89
3-pic	*cis*	1.52	1.33	1.72	3.35	1.98
3,4-lut	*cis*	1.70	1.19	1.76	3.34	2.00
3,5-lut	*cis*	1.46	1.27	1.67	3.31	1.93
	trans	2.68	1.24	0.19	3.33	1.86
Ave. gr. 1	*cis*	*1.47*	*1.31*	*1.68*	*3.35*	*1.95*
	trans	*2.68*	*1.24*	*0.19*	*3.33*	*1.86*
2,3-lut	*cis*	1.07	1.20	1.71	3.08	1.77
	trans	2.61	1.20	0.13	3.23	1.80
2,4-lut	*cis*	0.80	1.16	1.45	3.02	1.61
2,5-lut	*cis*	0.86	1.19	1.56	3.00	1.65
2,3,5-col	*cis*	0.66	1.14	1.82	3.00	1.66
Ave. gr. 2	*cis*	*0.85*	*1.17*	*1.64*	*3.03*	*1.67*
	trans	*2.61*	*1.20*	*0.13*	*3.23*	*1.79*
2,6-lut	*trans*	2.44	1.10	0.11	3.06	1.68
2,4,6-col	*trans*	2.44	1.02	0.09	3.05	1.65
2,3,6-col	*trans*	2.49	1.05	0.10	3.10	1.69
Ave. gr. 3	*trans*	*2.46*	*1.06*	*0.10*	*3.07*	*1.67*
Total ave.	*cis*	*1.16*	*1.24*	*1.63*	*3.19*	*1.81*
Total ave.	*trans*	*2.53*	*1.12*	*0.12*	*3.15*	*1.73*

trans series, the $\delta(^{195}Pt)$ were found at lower fields for group 3 complexes (ave. −1982 ppm), while the ave. $\delta(^{13}C)$ of the four C atom of pm in group 3 complexes ($\Delta\delta = 1.67$ ppm) is at higher field than for the two other groups. Therefore the $–CH_3$ substituents on the Ypy group located in *trans* position influence the electron density on the pyrimidine ligand. The C2 and C6 atoms close to the binding site are the most affected.

Coupling with the ^{195}Pt isotope was rarely observed. The $^2J(^{195}Pt–^{13}C2)$ coupling constants could be calculated for the *cis* 3,4-lut and the *trans* 2,3,6-col complexes. These values are 14 and 15 Hz.

The $\delta(^{13}C)$ of the Ypy ligands in the complexes are shown in the Supplementary material, and the $\Delta\delta(^{13}C)$ values are shown in Table S1. The values are larger for the C atoms bonded to a methyl group and for the methyl groups located in *ortho* positions. It is not possible to compare the results, since the local effects caused by the methyl substituents at different positions are too important.

Very few couplings of the Ypy C atoms with the ^{195}Pt isotope were observed. In *cis*-Pt(3,4-lut)(pm)Cl the $^3J(^{195}Pt–^{13}C3,5)$ is 38 Hz, while it is 28 and 30 Hz, respectively, for the *trans* 2,6-lut and 2,4,6-col analogues. Therefore it seems again larger for the *cis* isomers. A $^3J(^{195}Pt–^{13}C2,6–Me)$ coupling of 23 Hz could be calculated in the *trans* 2,6-lut compound. These results are similar to the few values reported in the literature [9,12,13].

3.2. $Cl_2(Ypy)Pt(\mu\text{-}pm)Pt(Ypy)Cl_2$

3.2.1. Synthesis

The pyrimidine-bridged dimers (Ypy = 2-pic, 3-pic, 2,3-lut, 2,4-lut, 2,5-lut, 3,4-lut, 3,5-lut and 2,3,5-col) were synthesized from the aqueous reaction of $K[Pt(Ypy)Cl_3]$ with pm using a Pt:pm ratio of 2:1 in the presence of NaCl. After two days of reaction, the mixture contains *cis* and *trans* monomers and dimers of different geometries. The mixture was refluxed in dichloromethane for 5 to 34 days (depending on the Ypy ligand), until only one product was obtained. The mixture can be periodically monitered by ^1H NMR. The final product was characterized by IR and multinuclear magnetic resonance spectroscopy and identified as the pyrimidine-bridged dinuclear species $Cl_2(Ypy)Pt(\mu\text{-}pm)Pt(Ypy)Cl_2$.

The aqueous reaction of $K[Pt(Ypy)Cl_3]$ (Ypy = 2,6-lut, 2,3,6-col and 2,4,6-col) with pyrimidine in a 2:1 proportion produced the *trans–trans* dimer after 5 days. The product of the reaction with 2,3,6-col contained some decomposed product, which could be removed by dissolving in dichloromethane and filtering out the impurities.

3.2.2. IR spectroscopy

The symmetry of the pyrimidine ligand in the dinuclear species is identical to the one of free pm. The A_2 modes are not active in IR.

Table 7
IR bands (cm^{-1}) of free pm and pm in the complexes $Cl_2(Ypy)Pt(\mu\text{-}pm)Pt(Ypy)Cl_2$

Mode	pm [24d]	3-pic	2,3-lut	2,4-lut	2,5-lut	3,4-lut	3,5-lut	2,6-lut	2,4,6-col	2,3,6-col
8b	1576				1595sh	1592sh	1593w	1603s	1602s	1592sh
8a	1566	1557w		1560w	1557vw		1559w			
19b	1467	1465w	1466s			1461m	1473w			1463sh
19a	1403	1412w	1410s	1414w	1412m	1414m	1412w	1411s	1411m	1411
			1403m			1403m		1402		
3	1237		1232w			1225sh		1224w		
15	1161		1180w	1180w	1175w			1168m		1184m
10b	832	816sh	820s	790s	824s	800vs	818sh	825m	829m	822m
							799vs		820sh	
4	721	695m	681s	701w	699m	702w	704sh			
6a	676	683m		684m	684S	687m	683m	687s	684m	683s
ν(Pt–Cl)			342s	348vs	344vs	345s	349m	343s	358m	347vs

There are 22 active A_1, B_1 and B_2 modes, but only 9 were assigned (Table 7). The different assignments have already been discussed in the monomer section.

The stretching ν(Pt–Cl) are strong and only one band was observed between 342 and 358 cm^{-1}. These results strongly suggest a *trans–trans* geometry for these dinuclear species.

3.2.3. Multinuclear magnetic resonance spectroscopy

The compounds were studied by ^{195}Pt NMR in $CDCl_3$. The results are listed in Table 8. Only one resonance was observed for all the compounds indicating isomeric purity, which was also confirmed by ^{1}H and ^{13}C NMR spectroscopy.

For the same Ypy ligand, the δ(Pt) of the dinuclear compound is very close to the one of the *trans* monomer. It seems that the electron density on the Pt atom in the dinuclear species is the same as in the *trans* monomers. The results in Table 8 have been separated into three groups as discussed previously. The group 3 complexes containing YPy ligands with two $-CH_3$ substituents in *ortho* positions were found at lower fields (ave. −1979 ppm) than those of group 2 (ave. −1998 ppm) and group 1 (ave. −2004 ppm), as observed in the monomers. The solvent effect is responsible for this observation. Since the Ypy planar ring is mainly perpendicular to the Pt plane, the $-CH_3$ substituents are located on both sides of the square plane in the close environment of the Pt atom. These substituents reduce the approach of the molecules of solvent close to the metal center, thus reducing the electron density on the Pt atom. As a result, the δ(^{195}Pt) will be shifted to lower field for group 3 compounds. The complexes of group 2 are observed at intermediate field. The signals of the dinuclear complexes containing Ypy ligands with $-CH_3$ substituents in positions 2 and 3 are always observed at slightly lower field than the others of their respective group, as observed for the monomers.

In these pm-bridged species, the atoms H4 and H6 are equivalent (C_{2v} symmetry) and only 3 signals will be observed in ^{1}H and ^{13}C NMR (see Scheme 2).

The H2 signal of pm in these compounds is a singlet, while the signal of H4 and H6 is a doublet and H5 a triplet. This pattern was also reported in the ionic complex $[Cl(NH_3)_2Pt(\mu\text{-}pm)Pt(NH_3)_2Cl]Cl_2$ [6]. In $Cl_2(R_2SO)Pt(\mu\text{-}pm)Pt(R_2SO)Cl_2$ [8], the signal of H2 is a singlet, the one of H4,6 is a doublet of doublets and the one of H5 is a doublet of triplets. The latter doublets are due to coupling with H2. In our compounds $Cl_2(Ypy)Pt(\mu\text{-}pm)Pt(Ypy)Cl_2$, there were no proton coupling with H2, although it was observed in the monomers discussed above.

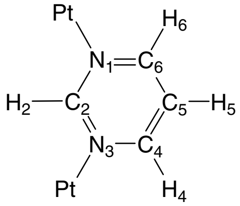

Scheme 2.

Table 8
δ(^{195}Pt) (ppm) of the compounds $Cl_2(Ypy)Pt(\mu\text{-}pm)Pt(Ypy)Cl_2$

Ypy	δ (ppm)	Ypy	δ (ppm)	Ypy	δ (ppm)
3-pic	−2005	2-pic	−2010	2,6-lut	−1990
3,4-lut	−2003	2,3-lut	−1984	2,4,6-col	−1984
3,5-lut	−2004	2,4-lut	−2005	2,3,6-col	−1962
		2,5-lut	−2008		
		2,3,5-col	−1982		
Ave. gr. 1	*−2004*	*Ave. gr. 2*	*−1998*	*Ave. gr. 3*	*−1979*

The Δδ(^{1}H) values of bonded pyridimine are shown in Table 9. The atom H2 is very shifted to lower field ($\Delta\delta_{ave.}$ = 1.09 ppm) as expected from the binding of its two neighbouring N atoms to two metal centers. The H4,6 atoms are also shifted similarly ($\Delta\delta_{ave.}$ = 0.66 ppm), while H5 is not very influenced by coordination ($\Delta\delta_{ave.}$ = 0.04 ppm).

The shifts towards lower fields are larger for group 3 compounds (ave. for C2 and C4,6, 1.123 and 0.702 ppm) than for group 2 (ave. 1.089 and 0.661 ppm) and group 1 (ave. 1.053 and 0.621 ppm) as reported above for the monomers. The Δδ values for H5 are small, much smaller than those reported in the series $Cl_2(R_2SO)Pt(\mu\text{-}pm)Pt(R_2SO)Cl_2$ ($0.291 \leqslant \Delta\delta \leqslant 0.381$ ppm) [8]. It seems that the presence of a strong π-accepting ligand (R_2SO) changes the electron density distribution on the pm-bridging ligand.

Table 9
Δδ(^{1}H) (ppm) for pm in $Cl_2(Ypy)Pt(\mu\text{-}pm)Pt(Ypy)Cl_2$

Ypy	H2	H4,6	H5	^3J(Pt–H2)	^3J(Pt–H4,6)
3-pic	1.055	0.626	0.051	18	27
3,4-lut	1.048	0.619	0.026	18	
3,5-lut	1.056	0.619	[a]	17	33
Ave. Gr. 1	*1.053*	*0.621*	*0.039*	*18*	30
2-pic	1.095	0.669	0.050	21	33
2,3-lut	1.097	0.669	0.041	21	31
2,4-lut	1.074	0.652	0.026	21	33
2,5-lut	1.093	0.658	0.041	22	33
2,3,5-col	1.088	0.657	0.033	19	37
Ave. Gr. 2	*1.089*	*0.661*	*0.038*	*21*	*35*
2,6-lut	1.128	0.706	0.037	20	33
2,4,6-col	1.110	0.693	0.015	19	29
2,3,6-col	1.132	0.708	[a]	20	
Ave. Gr. 3	*1.123*	*0.702*	*0.026*	*20*	31

[a] Hidden by H4 of YPy.

The coupling constants $^3J(^{195}Pt-^1H4,6)$ vary between 27 and 37 Hz and the $^3J(^{195}Pt-^1H2)$ are small (17–22 Hz), which seem to suggest a *trans–trans* geometry. A value of 15.8 Hz was reported in the literature for $^3J(^{195}Pt-^1H2)$ in *trans,trans*-$Cl_2(PBu_3)Pt(\mu\text{-pm})Pt(PBu_3)Cl_2$ [11]. In the $Cl_2(R_2SO)Pt(\mu\text{-pm})Pt(R_2SO)Cl_2$ series [8], $^3J(^{195}Pt-^1H2)$ varies from 20 to 24 Hz for the *trans–trans* species and between 25 and 26 Hz for the *cis–cis* isomers, while the constants $^3J(^{195}Pt-^1H6)$ are between 28 and 32 Hz for the *trans–trans* compounds and between 40 and 42 Hz for the *cis–cis* analogues. All these results strongly suggest a *trans–trans* geometry for our novel compounds $Cl_2(Ypy)Pt(\mu\text{-pm})Pt(Ypy)Cl_2$.

The $\Delta\delta(^1H)$ values of Ypy in the dinuclear compounds are shown in Table S2. The results are close to those observed for the *trans* monomers. The largest $\Delta\delta$ values are for the methyl substituents located in *ortho* positions. The same trend is also observed for the three groups of complexes. The coupling constants $^3J(^{195}Pt-^1H6)$ are between 28 and 33 ppm.

The $\Delta\delta(^{13}C)$ values of pm in these complexes are shown in Table 10. The latter are very large for C2 ($\Delta\delta_{ave} = 5.69$ ppm), smaller for C4,6 ($\Delta\delta_{ave} = 4.13$ ppm), while C5 is not affected by coordination ($\Delta\delta_{ave} = 0.13$ ppm).

Table 10 shows that the ave. $\Delta\delta(^{13}C)$ value for each group of complexes decreases from group 1 to group 3. These results are in agreement with those observed in ^{195}Pt NMR, where group 3 compounds were observed at lowest fields. In ^{13}C NMR, the C atoms of pm were observed at highest field for the group 3 compounds. When there is a reduction of electron density on the Pt atom ($\delta(^{195}Pt)$ at lower field), there is an increase of electron density on the pm ligand ($\delta(^{13}C)$ at higher field).

The $\delta(^{13}C)$ of the Ypy ligands are shown in the Supplementary material and the $\Delta\delta(^{13}C)$ values are listed in Table S3. The results are very similar to those observed for the *trans* monomers.

Coupling of the pm C atoms with ^{195}Pt are rarely observed. The 2,3-lut compound showed a $^3J(^{195}Pt-^{13}C5)$ of 25 Hz, while a few $^2J(^{195}Pt-^{13}C4,6)$ (13–15 Hz) could be evaluated (Table 11). Several $^3J(^{195}Pt-^{13}C)$ coupling were observed for the Ypy ligands, also shown in Table 11. The largest are with the C atoms located in *meta* positions (23–33 Hz), followed by the coupling with the methyl groups located in *ortho* positions (23–27 Hz). The couplings $^2J(^{195}Pt-^{13}C)$ are between 14 and 21 Hz and finally the couplings $^4J(^{195}Pt-^{13}C_{para})$ are 9 and 14 Hz. These values are consistent with a *trans–trans* geometry, although there are very few such data in the literature.

3.3. Crystal structures

The crystal structures of *cis*-$Pt(2,4\text{-lut})(pm)Cl_2$ (**1**), *trans*-$Pt(2,6\text{-lut})(pm)Cl_2$ (**2**) and *trans,trans*-$Cl_2(2,6\text{-lut})Pt(\mu\text{-pm})Pt(2,6\text{-lut})Cl_2$ (**3**) were determined by X-ray diffraction methods. The results have confirmed the configuration of the three compounds. The crystallographic data (Table 12) are slightly less precise for crystal **2**, which was found to be twinned. The *trans–trans* pyrimidine-bridged complex (**3**) contains a twofold axis and the atoms C2 and C5 of pyrimidine are located on the axis. It contains also 2 molecules of $CHCl_3$ per dimer. The conformation of the different molecules are shown on the labelled diagrams of the three compounds (Figs. 1–3).

The coordination around the Pt(II) atoms is square planar and the angles are close to the expected values. The Pt–Cl distances are normal (2.2945(9) - 2.3079(7) Å), while the Pt–N bonds are similar in the three crystals and they vary between 2.012(9) and 2.0228(18) Å. There is no difference between the bonds located in *trans* position to a chloro ligand or to a N-bonded ligand. These values agree with similar distances in the literature [8,12,14,25]. The Pt–N (pm) bonds (ave. 2.018(4) Å) do not seem shorter than the Pt–N (Ypy) bonds (ave. 2.021(4) Å).

Table 10
$\Delta\delta(^{13}C)$ (ppm) of pm in $Cl_2(Ypy)Pt(\mu\text{-pm})Pt(Ypy)Cl_2$

Ypy	C2	C4,6	C5	Ave.
3-pic	5.99	4.39	0.23	3.75
3,4-lut	5.97	4.31	0.22	3.70
3,5-lut	5.99	4.31	0.20	3.70
Ave. gr. 1	*5.98*	*4.37*	*0.22*	*3.72*
2-pic	5.68	4.18	0.16	3.55
2,3-lut	5.73	4.20	0.17	3.58
2,4-lut	5.63	4.10	0.14	3.49
2,5-lut	5.69	4.12	0.14	3.52
2,3,5-col	5.74	4.13	0.15	3.54
Ave. gr. 2	*5.69*	*4.15*	*0.15*	*3.54*
2,6-lut	5.39	3.91	0.04	3.31
2,4,6-col	5.40	3.85	0.00	3.28
2,3,6-col	5.45	3.91	0.04	3.33
Ave. gr. 3	*5.41*	*3.89*	*0.03*	*3.31*

Table 11
$J(^{195}Pt-^{13}C)$ values (Hz) observed in $Cl_2(Ypy)Pt(\mu\text{-pm})Pt(Ypy)Cl_2$

	3,4-lut	3,5-lut	2-pic	2,3-lut	2,4-lut	2,5-lut	2,6-lut	2,4,6-col
$^3J(Pt-C-Me_{ortho})$			26	24	23	24	26	27
$^3J(Pt-C_{meta})$	30	25	23	33	27/27	33/27	28	23
$^2J(Pt-C_{ortho})$		21		14		15/17		
$^4J(Pt-C_{para})$		9					14	
$^2J(Pt-C4,6\ pm)$			14	13		15		
$^3J(Pt-C5\ pm)$				25				

Table 12
Bond distances and angles

	cis-$Pt(2,4\text{-lut})(pm)Cl_2$ (**1**)	*trans*-$Pt(2,6\text{-lut})(pm)Cl_2$ (**2**)	$\{PtCl_2(2,6\text{-lut})\}_2(\mu\text{-pm})$ (**3**)[a]
Pt–Cl	2.2945(9) 2.3021(10)	2.2961(14) 2.3069(15)	2.3014(7) 2.3079(7)
Pt–N1	2.018(3)	2.012(9)	2.0228(18)
Pt–N2	2.021(3)	2.022(8)	2.0206(18)
N2–C (ave.)	1.352(4)	1.364(11)	1.358(3)
C–C (ave. Ypy)	1.380(5)	1.383(11)	1.379(4)
$C-CH_3$ (ave.)	1.498(5)	1.498(9)	1.489(4)
N1–C2	1.338(5)	1.361(12)	1.330(2)
N1–C6	1.342(5)	1.353(13)	1.352(3)
N3–C2	1.318(6)	1.326(9)	
N3–C4	1.324(6)	1.331(10)	
C4–C5	1.363(6)	1.398(15)	
C5–C6	1.367(5)	1.360(15)	1.376(3)
C1–Cl (ave.)			1.760(3)
Cl1–Pt–Cl2	93.35(4)	178.63(6)	177.89(3)
Cl1–Pt–N1	177.16(8)	90.3(2)	90.036
Cl1–Pt–N2	88.18(8)	89.89(19)	88.71(5)
Cl2–Pt–N1	89.20(9)	89.0(2)	90.41(6)
Cl2–Pt–N2	176.65(8)	90.8(2)	90.80(5)
N1–Pt–N2	89.21(11)	177.8(2)	178.20(7)
C12–N2–C16	118.9(3)	119.5(7)	120.4(2)
Pt–N2–C (ave.)	116.1(2), 125.0(2)	120.3(6)	119.73(15)
$N2-C-CH_3$ (ave.)	118.6(3)	118.4(6)	118.6(2)
$N2-C-C_{meta}$ (ave.)	119.8(3), 122.9(3)	120.8(7)	120.1(2)
C–C–C (ave. Ypy)	119.4(3)	119.7(8)	119.8(2)
$C-C-CH_3$ (ave.)	121.4(4)	120.9(6)	
Pt–N1–C2	120.6(3)	119.3(6)	118.03(16)
Pt–N1–C6	122.9(2)	123.3(7)	123.75(16)
C2–N1–C6	116.5(3)	117.3(9)	118.2(2)
N1–C2–N3	125.5(4)	125.1(7)	124.3(3)
N1–C6–C5	121.4(4)	120.6(10)	120.3(2)
C2–N3–C4	116.6(4)	116.8(6)	
N3–C4–C5	122.8(4)	122.0(7)	
C6–C5–C4	117.1(4)	119.1(10)	118.7(3)
Cl–C1–Cl (ave.)			110.23(15)

[a] Labelling on crystal **3** is slightly different for the pm ligand, which contains a twofold axis.

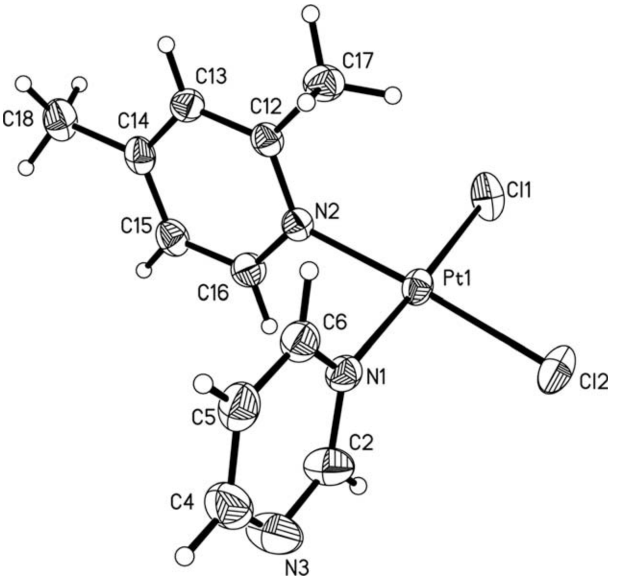

Fig. 1. Labelled diagram of *cis*-Pt(2,4-lut)(pm)Cl_2, (**1**). The ellipsoids correspond to 40% probability.

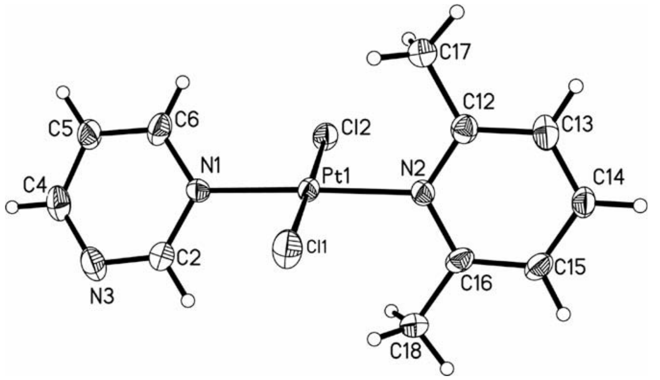

Fig. 2. Labelled diagram of *trans*-Pt(2,6-lut)(pm)Cl_2 (**2**). The ellipsoids correspond to 40% probability.

For the pyridine derivative, the ave. Pt–N2–C angles are 120.3(6) (**2**) and 120.4(2)° (**3**) for the compounds containing 2,6-lutidine. For crystal **1** which contains 2,4-lutidine, the external angle with C12, which is bonded to a $-CH_3$ substituent is larger (125.0(2)°) than the Pt–N2–C16 angle (116.1(2)°). The presence of $-CH_3$ groups reduces the internal C–C–C angles, as observed in the angle C13–C14–C15 in the 2,4-lut crystal (**1**) (117.1(3)°). In the same compound, N2–C12–C13 is smaller (119.8(3)°) than the N2–C16–C15 angle (122.9(3)°).

The ave. Pt–N1–C2 angles in the pyrimidine are smaller 118.03(16) to 120.6(3)° than the Pt–N1–C6 angles 122.9(2) to 123.75(16)°. In the monomers, the ave. N1–C bond distance is slightly longer (1.348(9) Å) than the N3–C bonds (ave. 1.325(8) Å). In the dimer where the two N atom are bonded to Pt, these distances are identical by symmetry (ave. 1.346(7) Å). The C–C distances are slightly longer (ave. 1.373(8) Å). These distances are in agreement with those determined in free pyrimidine (1.33(1) and 1.37(1) Å, respectively) [28]. The internal angles N–C–C (ave. 121.3(5)°) and N1–C2–N3 angles (ave. 125.0(3)°) are larger than the C–N1/3-C (ave. 117.3(4)°) and C–C–C angles (ave. 118.3(6)°). All these angles are similar to those of the free ligand [28] and the values reported in *trans*-Pt(pm)$_2X_2$ [10], Pt(R_2SO)(pm)X_2 [12–14] and in Cl_2(R_2SO)Pt(μ-pm)Pt(R_2SO)Cl_2 [8]. The binding of the N to the Pt atom does not change the internal angle at the N atom as it does in the hydrochlorides of pyrimidine and pyrimidin-2-one [29,30]. The protonation at N1 in the latter compounds increased the ring angle at the N atom by about 6°. This effect is not observed when Pt is the exocyclic bonded group. In the monomers (crystals **1** and **2**) the angles C–N1–C and C–N3–C are identical. Therefore, contrary to protonation, coordination to the platinum atom does not affect the structure of the pyrimidine ligand. For the pyrazine ligand, different results were reported. In *cis*- and *trans*-Pt(Ypy)(pyrazine)Cl_2 [31], the binding of pyrazine to platinum through the N1 atom slightly increased the internal C–N1–C angle, (ave. 117.6(3)°), while the non-bonded angle C–N4–C (ave. 115.6(3)°) is identical to the one in free pyrazine (115.1°) [32]. In the two Pt-pyrazine compounds, the N1–C–C angles are smaller (ave. 120.5(3)°) than the N4–C–C angles (ave. 123.1(4)°). In free pyrazine, these angles are 122.4° [32].

Planar ligands such as pyridine derivatives and pyrimidine are often perpendicular to the platinum plane in order to reduce the steric hindrance, especially for *ortho*-substituted pyridine ligands. For 2,6-lutidine, the most stable conformer is the one where the ligand is perpendicular to the Pt plane. The orientation of the planar rings is particularly important in *cis* isomers, where steric factors are usually very important. For *cis*-Pt(2,4-lut)(pz)Cl_2, where the Ypy ligand contains one *ortho* substituent, the dihedral angle between the platinum and the pyrimidine planes is 70.13(9)°, while the angle between the Pt and the 2,4-lutidine plane is 80.73(7)°. In the *trans* geometry, these angles should be smaller. For *trans*-Pt(2,6-lut)-(pz)Cl_2, where the Ypy ligand contains two *ortho* substituents, the dihedral angle between the Pt(II) plane and the 2,6-lutidine plane is 76.38(15)°, while the angle between the Pt(II) and pyrimidine

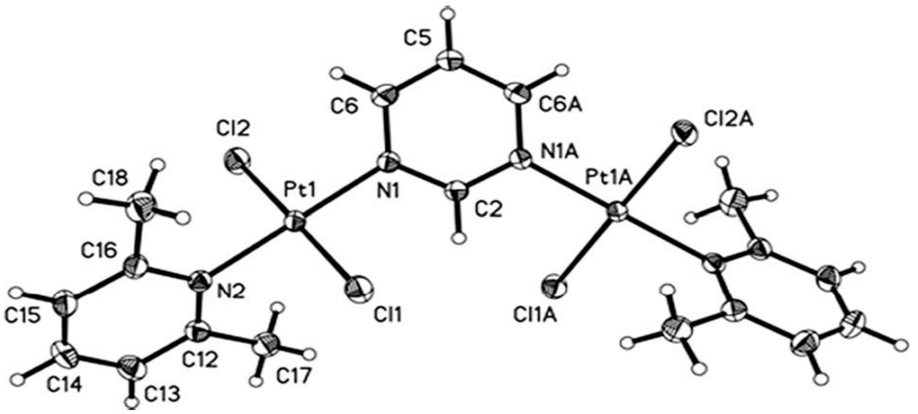

Fig. 3. Labelled diagram of *trans,trans*-Cl_2(2,6-lut)Pt(μ-pm)Pt(Ypy)Cl_2 (**3**). The ellipsoids correspond to 40% probability.

planes is 60.12(15)°. In the pyrimidine-bridged dimer, the dihedral angle between the Pt(II) and the 2,6-lut planes is much larger (87.98(6)°) than the one between the Pt(II) and pyrimidine planes (43.97(9)°).

Packing forces are probably the more determining factors in the orientation of the pyrimidine or pyridine rings, when there is no important steric hindrance. It has also been suggested that the presence of π-bonding between Pt(II) and the aromatic ligand would tend to decrease this angle [23]. An intermediate angle would be a compromise between the two factors, steric hindrance, which would tend to increase the dihedral angle and more effective Pt–N π-bonding, which would tend to reduce the angle. We are not suggesting that π-bonding is very important in these types of complexes, but it might be present, since pyridine and pyrimidine contains empty π^* orbitals, which can accept electron density from a soft metal like Pt(II). Therefore, when steric factors are less important, the orientation of these planes results from several smaller factors.

The dinuclear species (**3**) crystallized with two molecules of chloroform per dimer. It does not seem to influence the structure of the Pt(II) molecule. The average C–Cl distance is 1.760(3) Å and the average angle Cl–C–Cl is 110.23(15)°.

4. Conclusion

Novel mixed-ligand Pt(II) complexes containing pyrimidine and a pyridine derivative were synthesized and characterized in the solid state by IR spectroscopy and in solution by multinuclear magnetic resonance spectroscopy. Monomers of the types *cis*- and *trans*-Pt(Ypy)(pm)Cl_2 and pyrimidine-bridged dinuclear species Cl_2(Ypy)Pt(μ-pm)Pt(Ypy)(pm)Cl_2 were studied. The *cis* monomers containing Ypy with two –CH_3 substituents in *ortho* position cannot be synthesized because of steric hindrance. The *cis* monomers, the *trans* monomers containing Ypy with two methyl substituents in *ortho* positions and the dinuclear compounds were prepared pure, while the other *trans* monomers contain other species. The latter compounds were prepared from the isomerization of the *cis* isomers in dichloromethane. The *cis* → *trans* isomerization is very slow and the product is usually contaminated with the pm-bridged dimer and other species such as *trans*-Pt$(pm)_2Cl_2$ and *trans*-Pt$(Ypy)_2Cl_2$. IR and NMR spectroscopies indicated strongly that the dinuclear species have the *trans–trans* geometry.

The NMR results were interpreted in relation to the solvent effect. For each series of complexes, the compounds were classified into three groups depending on the Ypy ligand. Group 1 complexes contains pyridine derivatives which have no –CH_3 substituent in *ortho* position, group 2 includes Ypy which have one –CH_3 substituent in *ortho* position, while group 3 contains the Ypy ligands which have two –CH_3 substituents in *ortho* positions. The solvent normally weakly binds the metal atom on both sides of the square plane, which increases the electron density on the metal center. Planar ligands such as pyridine derivatives are usually perpendicular to the square plane in order to reduce steric hindrance with the *cis* neighbours. This is particularly true when the pyridine derivative contains –CH_3 substituents in *ortho* positions. In this conformation, the –CH_3 substituents are directly on top and bottom of the coordination plane, thus preventing the approach of the molecules of solvent towards the Pt atom. The presence of these substituents will therefore reduce the electron density on the metal center, reflected by a downfield shift in ^{195}Pt NMR.

The $\delta(^{195}Pt)$ of group 1 complexes were observed at highest fields, while the group 3 compounds were found at lowest fields for the three series of new compounds (the *cis* and *trans* monomers and the *trans–trans* dinuclear species). The $\delta(^{13}C)$ of the pyrimidine C atoms of the three groups of compounds are in the reverse order as expected. When the electron density on the Pt atom increases, there is an electron density reduction on the pm ligand. The influence of the –CH_3 substituents in *ortho* positions of the pyridine ligand was also observed in ^{1}H NMR.

Several couplings of the types $J(^{195}Pt–^1H)$ and $J(^{195}Pt-^{13}C)$ are reported. The ^3J values are always larger in the *cis* compounds than in the *trans* isomers. A few ^2J and ^4J are also reported. These values are quite small.

The crystal structures of three compounds were determined by crystallographic methods. The results have confirmed the configurations suggested by IR and multinuclear magnetic resonance spectroscopies for the three new types of Pt(II) compounds.

Acknowledgment

The authors are grateful to the Natural Sciences and Engineering Engineering Research Council of Canada for financial support of the project.

Appendix A. Supplementary material

CCDC 689624, 689625 and 689626 contain the supplementary crystallographic data for this paper. These data can be obtained free of charge from The Cambridge Crystallographic Data Centre via www.ccdc.cam.ac.uk/data_request/cif. The supplementary material includes a list of the NMR spectra of the complexes, $\Delta\delta(^{13}C)$ (ppm) for Ypy in Pt(Ypy)(pm)Cl_2 (Table S1), the $\Delta\delta(^1H)$ (ppm) of Ypy in Cl_2(Ypy)Pt(μ-pm)Pt(Ypy)Cl_2 (Table S2) and the $\Delta\delta(^{13}C)$ (ppm) for Ypy in Cl_2(Ypy)Pt(μ-pm)Pt(Ypy)Cl_2 (Table S3). Supplementary data associated with this article can be found, in the online version, at doi:10.1016/j.ica.2008.07.003.

References

[1] T.W. Hambley, Coord. Chem. Rev. 166 (1997) 181.
[2] E.R. Jamieson, S. Lippard, J. Chem. Rev. 99 (1999) 2467.
[3] N. Farrell, T.B.T. Ha, J.P. Souchard, F.L. Wimmer, S. Cros, N.P. Johnson, J. Med. Chem. 32 (1989) 2240.
[4] Y. Chen, Z. Guo, J.A. Parkinson, S. Parsons, P.J. Sadler, Chem. Eur. J. 4 (4) (1998) 672.
[5] J. Holford, F. Raynaud, B.A. Murrer, K. Grimaldi, J.A. Hartley, M. Abrams, L.R. Kelland, Anti-Cancer Drug Des. 13 (1998) 1.
[6] S. Komeda, G.V. Kalayda, M. Lutz, A.L. Spek, Y. Yamanaka, T. Sato, M. Chikuma, J. Reedijk, J. Med. Chem. 46 (2003) 1210.
[7] (a) N.J. Wheate, J.G. Collins, Coord. Chem. Rev. 241 (2003) 133;
(b) S. Komeda, M. Lutz, A.L. Spek, M. Chikuma, J. Reedijk, Inorg. Chem. 39 (2000) 4230;
(c) S. Komeda, M. Lutz, A.L. Spek, Y. Yamanaka, T. Sato, M. Chikuma, J. Reedijk, J. Am. Chem. Soc. 124 (2002) 4738.
[8] N. Nédélec, F.D. Rochon, Inorg. Chem. 40 (2001) 5236.
[9] G.V. Fazakerley, K.R. Koch, Inorg. Chim. Acta 36 (1979) 13.
[10] F.D. Rochon, P.-C. Kong, R. Melanson, Can. J. Chem. 59 (1981) 195.
[11] W. Kaufmann, L.M. Venanzi, A. Albinati, Inorg. Chem. 27 (1988) 1178.
[12] N. Nédélec, F.D. Rochon, Inorg. Chim. Acta 319 (2001) 95.
[13] F.D. Rochon, G. Masserweh, N. Nédélec, Inorg. Chim. Acta 346 (2003) 197.
[14] F.D. Rochon, C. Tessier, Inorg. Chim. Acta 361 (2008) 2591.
[15] APEX 2, Version 2.0.2, Bruker AXS Inc., Madison, WI, USA, 2005.
[16] SAINT, Version 7.07a, Bruker AXS Inc., Madison, WI, USA, 2003.
[17] G.M. Sheldrick, SADABS, Version 2004/1, Bruker AXS Inc., Madison, WI, USA, 2004.
[18] G.M. Sheldrick, SHELXS-97 and SHELXL-97, Programs for the Refinement of Crystal Structures, University of Gottingen, Germany, 1997.
[19] A.J.C. Wilson (Ed.), International Tables of Crystallography, vol. C, Kluwer Academic Publishers, Dordecht, 1992 (Tables 4.2.6.8 and 6.1.1.4).
[20] SHELXTL, Version 6.12, Bruker AXS Inc., Madison, WI, USA, 2001.
[21] A.L. Spek, PLATON, A Multipurpose Crystallographic Tool, Universiy of Utrecht, Utrecht, The Netherlands, 2005.
[22] P.-C. Kong, F.D. Rochon, Can. J. Chem. 56 (1978) 441.
[23] F.D. Rochon, A.L. Beauchamp, C. Bensimon, Can. J. Chem. 74 (1996) 2121.
[24] (a) L.C. Lord, A.L. Martson, F.A. Millers, Spectrochim. Acta 9 (1957) 113;
(b) A. Navarro, M. Fernandez-Gomez, J.J. López-González, M.P. Fernández-Liencres, E. Martinez-Torres, J. Tomkinson, G.J. Kearl, J. Phys. Chem. A 103 (1999) 5833;
(c) A.D. Boese, J.M.L. Martin, J. Phys. Chem. A 108 (2004) 3085;
(d) S. Breda, I.D. Reva, L. Lapinski, M.J. Nowak, M.R. Fausto, J. Mol. Struct. 786 (2006) 193;
(e) M. Pfeffer, P. Braunstein, J. Dehand, Spectrochim. Acta 30A (1974) 331;

(f) J.H.S. Green, D.J. Harrison, W. Kynaston, H.M. Paisle, Spectrochim. Acta 26A (1970) 2139;
(g) V.I. Berezin, M.D. Él'Kin, Russ. Phys. J. 15 (3) (1972) 462;
(h) J.H. Green, D.J. Harrison, Spectrochim. Acta 29A (1973) 293.
[25] C. Tessier, F.D. Rochon, Inorg. Chim. Acta 295 (1999) 25.
[26] W.G. Fatley, F.R. Dollish, N.T. McDevitt, F.F. Bentley, Infrared and Raman Selection Rules for Molecular and Lattice Vibrations: The Correlation Method, Wiley-Interscience, New York, 1972.
[27] D.D. Derrin, Dissociation Constants of Organic Bases in Aqueous Solution, Butterworth, London, 1965, pp. 140–183.
[28] P.J. Wheatley, Acta Crystallogr. 13 (1960) 80.
[29] S. Furberg, J.B. Aas, Acta Chem. Scand. A 29 (1975) 713.
[30] C. Singh, Acta Crystallogr. 19 (1965) 861.
[31] F.D. Rochon, M. Fakhfakh, Inorg. Chim. Acta 362 (2009) 458.
[32] P.J. Wheatley, Acta Crystallogr. 10 (1957) 182.